Journal of Nuclear Materials 385 (2009) 591–594

Contents lists available at ScienceDirect

Journal of Nuclear Materials

journal homepage: www.elsevier.com/locate/jnucmat

Effect of hydrogen on the creep behavior of Zr–2.5%Nb alloy at 723 K

R. Kishore *

Mechanical Metallurgy Section, Materials Group, B.A.R.C., Trombay, Mumbai 400 085, India

ARTICLE INFO

Article history:
Received 20 August 2008
Accepted 8 January 2009

ABSTRACT

Increased plasticity is reported in Ti alloys, stainless steels and Pd by the introduction of hydrogen. The dissolved hydrogen in zirconium and its alloys which have similar properties as those of titanium and its alloys, can modify the creep properties of the matrix. Hydrogen, formed during the corrosion reaction of Zr–2.5%Nb pressure tube, in a CANDU design nuclear reactor, with the coolant can ingress into the metal matrix. This absorbed hydrogen can lead to an unexpected increase in length and in diameter of the pressure tube. In order to evaluate the effect of hydrogen on the creep behavior of the pressure tube material, tensile specimens with longitudinal and transverse orientations were hydrided to 65 and 160 wt ppm and creep tested at 723 K over a stress range. The combined influence of hydrogen and specimen orientations on creep rate is evaluated, and an attempt is made to explain the results using the deformation mechanisms reported in literature.

1. Introduction

Zirconium base alloys are the only materials which satisfy many unique requirements for use in nuclear power reactors. Among the various zirconium alloys developed over the years, the Zr–2.5wt%Nb alloy was found to have many advantageous properties. The latter alloy, besides having higher strength and better corrosion resistance over the earlier developed alloys, has lower hydrogen pick up. Hydrogen is known to influence the mechanical properties of zirconium alloys [1] and has been reported to increase the ductility in many materials. Though initial studies have indicated an increase in the yield and the flow stresses in iron and steels by the addition of hydrogen under uni-axial loading [2], a reduction in the torsional yield in a medium carbon steel is also reported [3]. Softening in pure Fe and some ferrous alloys were reported to occur by the addition of hydrogen [4–7]. In palladium, hydrogen was reported to increase the creep rate by six times in the temperature range of 736–1200 K [8]. Softening is reported to occur in Ti6Al4V, a group IV based alloy having properties similar to zirconium alloys, by the addition of hydrogen [9,10]. The creep strain, at room temperature, in another titanium alloy (Ti–5Al–2.5Sn) was reported to have increased (at smaller strains) by the additions of 100 wt ppm hydrogen [11]. In Zircaloy-4, an addition of 300 wt ppm hydrogen has been shown to slow down the rate of recovery and re-crystallization [12] which indirectly can influence the creep behavior. But the creep tests in annealed Zircaloy-2 at 300 °C containing hydrogen up to 1075 ppm did not show any deterioration in creep strength [13]. In Zircaloy-4, the creep behavior was reported to depend on the condition of the material – whether it is in cold-worked and stress relieved (CWSR) or in annealed condition [14,15]. In Zircaloy-4 cladding tubes under CWSR condition, a significant strengthening was reported with the addition of hydrogen. The creep strength of the same alloy under annealed condition was reported to show a decrease when the hydrogen was in solution and an increase when the part of the hydrogen precipitated as hydrides [15]. A recent study in zirconium and Zircaloy-4, using indentation technique, has indicated an increase in the creep rate with the addition of hydrogen [16]. The above studies imply that hydrogen can influence the creep behavior in zirconium alloys, which is a life limiting factor for nuclear components like pressure tube and fuel clad.

1.1. Pressure tube

A pressure tube under an operating coolant pressure of 10 MPa, experiences an axial stress of ∼60 MPa and a hoops stress of ∼120 MPa, assuming closed-end configuration. Thermal creep, irradiation creep and irradiation growth contribute to axial and transverse elongations and are well accepted life limiting phenomena in the case of pressure tube during service. As a first approximation, the rate of overall strain is taken as the sum of the rates of these three strains i.e. $\dot{\varepsilon}_T = \dot{\varepsilon}_{ir} + \dot{\varepsilon}_{gr} + \dot{\varepsilon}_{th}$ where, $\dot{\varepsilon}_{ir}$, $\dot{\varepsilon}_{gr}$, $\dot{\varepsilon}_{th}$ are the strain rates due to irradiation, growth and thermal creep, respectively. Thermal creep predominates at either ends of the pressure tube where the neutron flux is low and irradiation creep dominates in the middle. Provisions are made in the PHWR (Pressurized Heavy Water Reactor) design to allow the increase in the length of the pressure tube. Increase in the diameter of the pressure tube causes inadequate cooling of the fuel bundles leading to attaining a premature thermal hydraulic limit. The important parameters that affect the creep of in-reactor pressure tubes are the crystallographic

---

* Tel.: +91 22 2559 3814.
E-mail address: kishorer@barc.gov.in

0022-3115/$ - see front matter © 2009 Elsevier B.V. All rights reserved.
doi:10.1016/j.jnucmat.2009.01.034

texture, the chemical composition, the microstructure (involving the grain size, the volume fraction and distribution of second phase which varies from end-to-end of the 6 m long tube), the density and Burgers' vector of dislocations, the stress, the temperature and the neutron flux.

1.2. Fuel clad

In dry depository or during transport to reprocessing plants, the clad temperature can reach well over 400 °C in 10 days of removal from the reactor [12]. This is all the more important for high burn-up fuel rods. The cladding is subjected to high internal pressure due to fission gases and helium. Though high performance Zr based HANA (High performance Alloy for Nuclear Application) alloys [17] are being developed with better creep resistance than Zircaloy-4, an evaluation of the creep properties of these alloys as a function of various material variables is necessary.

The pressure tube and clad material pick up hydrogen during service. An important problem in zirconium alloys which has received only a limited attention is the effect of hydrogen on the creep behavior of this material. In the case of pressure tube, the hydrogen pick up rate can vary from channel to channel. The variation in pick up rate arises from, besides the prevailing corrosion conditions, the variations in the composition of the alloy, in the texture of the pressure tube, in the distribution and volume fraction of the second phase (β) etc. This can lead to a difference in the creep rate (axial) between adjacent channels, assuming that the creep deformation in out-of-pile and in-reactor conditions are affected by the various parameters listed above in the same way. This differential elongation can lead to a reduction in the distance between their feeder pipes to dangerous values.

In this paper, preliminary results of the studies on the effect of hydrogen on the creep behavior in Zr–2.5%Nb pressure tube material are presented. Tensile specimens were machined from the cold pilgered and stress relieved pressure tube in longitudinal and transverse orientations. These specimens were hydrided to 65 and 160 wt ppm level and creep strain measurements at 723 K over a stress range of 25–150 MPa are presented. The results are explained on the basis of existing models.

2. Experimental details

2.1. Material

The Zr–2.5%Nb alloy was received in the form of cold pilgered and stress relieved (final) condition. The nominal composition of the Zr–2.5%Nb material used in this investigation is shown in Table 1. The concentration of hydrogen is kept at lowest level in order to reduce its embrittling effects on the material [18]. The fabrication procedure of the pressure tube [19] and the method of hydriding the experimental specimens are covered elsewhere [20]. The tube has a strong basal pole texture in the transverse direction, with a basal pole fraction of 0.683 in the hoops direction and 0.098 in the axial direction. Tensile specimens with a gage length of 25 mm were machined from the tube such that the tensile axis for one set of specimens is parallel to the longitudinal direction and for a second set it is parallel to the transverse direction of the tube. The tube sections were cold flattened before transverse specimens were machined. The longitudinal and transverse specimens were machined from the pressure tube from locations as close as possible to keep the scatter in mechanical properties low. The oxide layer was removed by grinding and polishing. Care was taken to remove the grease or oil stains from the specimen surface. The samples were hydrided in a gaseous charging system at 623 K to two hydrogen levels of about 80 and 185 wt ppm. All the specimens (as received and hydrided) were subsequently stress relieved (annealed) at 673 K for 72 h under 100 mm helium pressure. The final hydrogen content was estimated by vacuum fusion technique. The analyses are shown in Table 1 and the estimated values were taken to represent the true hydrogen content.

Table 1
Nominal composition (%wt) of the Zr–2.5%Nb pressure tube alloy.

Nb	O (wt ppm)	H (wt ppm)	N (wt ppm)	Sn	Cr	Fe	Ni	Zr
2.53	1200	5	5	0.018	0.020	0.13	<0.007	Bal

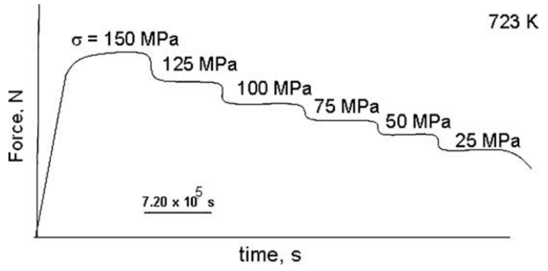

Fig. 1. Schematic of the creep test procedure followed in this investigation.

2.2. Creep tests

The specimens were tested in a constant load lever arm creep machine and the furnace temperature was controlled so as to give a temperature of 723 ± 1 K on the sample. The specimens were soaked at this temperature for 1800 s before the commencement of the test. To start with, dead weights were placed on the lever pan such that a stress of 150 MPa was felt at the gage cross section of the specimen and the extension, as a function of time, was recorded. Once the steady creep state was achieved, the load was reduced and the specimen was allowed to attain a steady state at this load level. Such load decrements were followed till a stress level of 25 MPa was reached. A schematic load-time plot of the test schedule is shown in Fig. 1. Single specimen was used in the load decrement test so that the chemical composition and texture remain unaltered. All the tests were done in air. Such load decrement tests were performed on both the longitudinal and the transverse orientations of the specimens in as received and in the hydrided conditions. It must be mentioned here that such single specimen tests may not be able to reflect the variation in the creep behavior from end-to-end of the tube. The extension, measured using a LVDT having a resolution of 2 μm, was continuously recorded as a function of time throughout the course of the test.

3. Results and discussion

The hydrogen levels in the specimens are indicated in Table 2. Though the longitudinal and transverse specimens could not be hydrided exactly to the same concentration, the average values of 65 and 160 wt ppm are taken to represent the two hydrogen levels in the specimens (Table 2). The true stress and true strain were estimated from the applied load and the measured extension. The creep rate was calculated from the creep strain - time plot for all the all stress levels.

The creep rate ($\dot{\varepsilon}$) can be related to the applied stress (σ) by a power law relation:

$$\dot{\varepsilon} = A(\sigma/E)^{n}\exp(-Q/RT) \tag{1}$$

Table 2
The hydrogen levels in tensile specimens: (i) gaseous charged and (ii) estimated by vacuum fusion technique.

Sample	Charged level, wt ppm	Estimated (±2) wt ppm		
		Longitudinal	Transverse	Average (longitudinal or transverse)
1	As received	5	5	5
2	80	68	62	65
3	185	166	154	160

Table 3
The variation in n values for longitudinal and transverse orientation as a function of hydrogen content.

Hydrogen level, wt ppm	Longitudinal	Transverse
5	2.81	1.86
65	2.43	1.78
160	2.41	1.59

where n the stress exponent, A is a constant, Q the activation energy for creep and E the Young's modulus. The variation in creep rate with stress for the unhydride and hydrided specimens for both the orientations (longitudinal and transverse) is shown in Fig. 2 and the slopes of the regression lines give the stress exponents. It may be seen that the creep rate is higher for the hydrided sample and increases with the hydrogen content for both the orientations. The following points are clear from Fig. 2:

(a) Transverse creep rate, in general, are higher than axial creep rate – both in the unhydrided and in the hydrided conditions. This difference is due to the strong anisotropy in this material.
(b) Increase in hydrogen concentration causes the creep rate to increase, albeit by different magnitudes, in both the orientations (transverse and longitudinal).
(c) The stress exponent decreases with hydrogen content for both the orientations and this decrease is higher (i) for axial orientations at lower hydrogen levels and (ii) for transverse orientation at higher hydrogen levels (Table 3).

In the literature, hydrogen induced plasticity is attributed to different mechanisms. Matsui et al. [5–7] interpreted their results of decreased flow stress in hydrogenated iron to be due to decrease in energy to nucleate kinks on screw dislocations. Accordingly, hydrogen decreased the Peierls Nabarro force and increased the dislocation mobility. Oriani [21] proposed a threshold fugacity above which the stress relaxation and creep rate increased. This mechanism leads to formation of micro-voids at internal surfaces of the matrix. Another interpretation of hydrides contributing to the ductility was given by Paton and Thompson [11]. They attributed the increase in the creep rate to the punching of dislocation loops by newly formed hydrides which are associated with an increase in volume. The dissolved hydrogen in nickel and its alloys is reported to decrease the activation enthalpy in the system which aids to increase dislocation velocity [22]. With increased density and mobility of dislocations due to hydrogen addition, the material is rendered more ductile [22]. A decrease in activation volume has also been shown to induce softening at low strain levels [10]. The hydrogen atmosphere at the dislocation is expected to shield the core and reduces the interaction of dislocation with other dislocations or with other obstacles [23]. Under such conditions the dislocation interaction is reduced and dislocations are rendered mobile, resulting in higher creep rate.

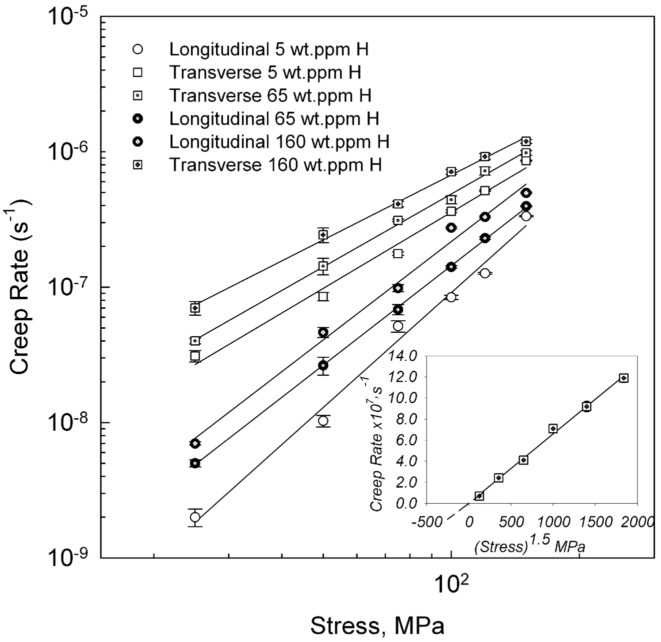

Fig. 2. Plot of creep rate against applied stress for longitudinally and transversely oriented specimens with different hydrogen contents. The scatter bars shown are the standard deviation values obtained when the creep rates are estimated from the strain-time plot. The inset is a typical re-plot for transverse orientation (160 wt ppm) and shows negligible threshold stress (on extrapolation).

Among the models cited above, the control of deformation by screw dislocation and hydrides punching glissile loops is not applicable to the present context as the deformation is at not occurring at low temperatures. The 160 wt ppm of hydrogen is below the solubility limit of hydrogen in zirconium at the test temperature (723 K) [24] and no hydrides are expected to form. It may be expected that the hydrogen atoms diffuse to dislocations to form a cloud and this local concentration is proportional to the nominal concentration in the matrix. As the nominal concentration of hydrogen in the matrix increases the interaction between dislocations gets reduced because of the shielding effect and the creep rate increases. Ab initio calculation by Rupa et al. [15] indicates that the hydrogen that segregates to the core of screw dislocation, modify the core and reduce the stacking fault energy. This results in the increased mobility of the partials which causes an increase in the creep rate. On the other hand, when the hydrides form they increased the internal stress and caused a hardening of the matrix [15]. Though this mechanism can explain the present results qualitatively, the following mechanism proposed by Daigo Setoyama et al. [16] is also relevant. The marginal increase in creep rate of zirconium and Zircaloy-4 at a test temperature of 693 K and a stress of 150 MPa with an addition of 200 wt ppm hydrogen is attributed to the decrease in the modulus value [16]. The modulus is reported to decrease with the addition of hydrogen and this can cause a reduction in the creep rate in accordance with Eq. (1). In this study, it may be noted from Fig. 2 that for a typical stress value of 100 MPa the creep rate increases from $9.5 \times 10^{-8}\ \mathrm{s}^{-1}$ (undydrided specimens) to $2.2 \times 10^{-7}\ \mathrm{s}^{-1}$ and from $3.6 \times 10^{-7}\ \mathrm{s}^{-1}$ (unhydrided specimen) to $7.0 \times 10^{-7}\ \mathrm{s}^{-1}$ for longitudinal and transverse specimens respectively for a hydrogen concentration of 160 wt ppm. This works out to an increase in the creep rate by ~2.3 and ~1.9 times for longitudinal and transverse specimens, respectively. If we use the modulus value and assume the same linear dependence of the modulus with hydrogen concentration as reported in Ref. [16] and estimate the ratio of the creep rate between the as received specimens (with 5 wt ppm) and the one with 160 wt ppm hydrogen, the increase is about 1.1 which is lower than those obtained from this experiments. This may be explained as follows.

The present alloy is two phase mixture of α (HCP) and β (BCC) at the test temperature and the former phase is harder than the latter. The β phase has higher solubility for hydrogen and the dissolved hydrogen gets redistributed between the two phases. The overall effect of hydrogen on the creep rate is the combined contribution from the two individual phases (α and β) with varying levels of hydrogen in them. In the absence of any data on the variation in the modulus value of the two phases with the addition of hydrogen, it is not possible to comment on the extent to which each of the phases contribute to the creep rate.

The *n* value: the stress exponent (*n*) for the unhydrided longitudinal sample was found to be 2.81, reduced to 2.43 for a hydrogen addition of 65 wt ppm and appeared to saturate around this value for further addition of hydrogen to 160 wt ppm (Table 3). The *n* value, in the case of transverse specimen, was noted to be 1.86 in the unhydrided condition which reduced with the addition of hydrogen and reached a value closer to 1.59 for a hydrogen level of 160 wt ppm. The *n* value obtained in this work is about 1/3 of that reported by Shewfelt [25] and closer to that reported by Chirstodolu et al. [26] for a similar alloy in the longitudinal orientation. The value of 2.81 obtained in this study, in the case of longitudinal specimen, indicates that dislocation glide is the possible deformation mechanism and the mechanism tends towards grain boundary sliding (2.41) with the addition of hydrogen. In the case of transverse specimens the mechanism tends to shift from grain boundary sliding to diffusional creep (from an *n* value of 1.86 to 1.59) with the addition of hydrogen. Though hydrogen is a β stabilizer, it is not possible to expect the volume fraction of β to increase considerably for the low levels of hydrogen discussed in this work and modify the deformation behavior. The creep mechanism in α-zirconium at low stresses is still not fully resolved as to diffusion controlled [27,28] or grain boundary sliding [29]. At higher stress, typical range used in this investigation, the reported creep mechanism is dislocation controlled for the longitudinal specimen [26]. It should be pointed out here that the *n* value was reported to be invariant with the addition of hydrogen for zirconium and Zircaloy-4 [16] whereas in the present case the *n* is found to decrease (Table 3). These *n* values get modified if threshold stresses (a stress value below which no measurable creep strain is noted) are present.

In order to verify the absence of a threshold stress, the slope from the $\dot{\varepsilon} - \sigma$, was measured (the stress exponent in Eq. (1)) and a re-plot of $\dot{\varepsilon} - \sigma^{n}$ was made on linear scale [27–29]. The inset in Fig. 2 shows such a typical plot for the transverse specimen with 160 wt ppm hydrogen. The absence of any measurable threshold values indicates that the *n* values measured from Fig. 2 remain unaltered.

A mention on the creep rate with respect to specimen orientation is necessary. It was reported [25] that the transverse orientation becomes softer over the longitudinal orientation at temperature above 823 K and the mechanism is attributed to grain boundary sliding. The present data also confirm the reverse trend (i.e. transverse orientation exhibiting higher creep rate than the longitudinal one) but at a lower temperature (723 K). This reduction in the temperature for the reversal possibly is due to the lower stress relieving treatment employed for the samples in this study (673 K/72 h) as compared to a higher temperature used in Ref. [25] (873 K) where the α grains are reported to have got equiaxed.

Though, it is not possible to arrive at a definite relation between the creep rate and hydrogen concentration with only two concentration values, this results indicate that the increase in creep rate can be positively correlated with the hydrogen content.

4. Conclusions

In Zr–2.5%Nb alloy containing 65 and 160 wt ppm hydrogen, the creep tests in the longitudinal and transverse direction of the pressure tube at 723 K reveal that

(1) The creep rates in the transverse and in the longitudinal directions increase by about 2–2.5 times with 160 wt ppm addition of hydrogen. The creep rate increases with the hydrogen concentration, within the range examined here.
(2) In unhydrided condition, a value of 2.8 for stress exponent in longitudinal direction indicates that the creep mechanism is dislocation controlled and a value of 1.86 in transverse specimen indicates that the mechanism is closer to grain boundary sliding. These values fall to 2.41 and 1.59 for longitudinal and transverse orientations, respectively with an addition of 160 wt ppm hydrogen, indicating a change in the deformation mechanism.

Acknowledgement

The author likes to thank Dr M. Sundararaman (BARC) for the critical reading of this article and his expert comments. The author is highly grateful to the unknown reviewer who has brought out some important points to the fore which helped the author to improve the manuscript.

References

[1] J.-H. Huang, S.-P. Huang, J. Nucl. Mater. 208 (1994) 166.
[2] S. Asano, R. Otsuka, Scr. Metall. 12 (1978) 287.
[3] C.D. Beachem, Metall. Trans. 3 (1972) 437.
[4] I.M. Bernstein, Scr. Metall. 8 (1974) 343.
[5] H. Matsui, H. Kimura, Mater. Sci. Eng. 40 (1979) 217.
[6] H. Matsui, S. Moriya, H. Kimura, Mater. Sci. Eng. 40 (1979) 207.
[7] H. Matsui, S. Moriya, S. Takaki, H. Kimura, Trans. Japan Inst. Metals 19 (1978) 163.
[8] Z.R. Xu, R.B. Mclellan, Acta Mater. 46 (1998) 4543.
[9] X.J. Wan, G.Y. Gao, Proceedings of the 5th National Cong Titanium Alloys, China, 1984.
[10] G.Y. Gao, S.C. Dexter, Metall. Trans. 18A (1987) 1125.
[11] N.E. Paton, A.W. Thompson, Metall. Trans. 13 (1982) 1531.
[12] J. Dunlop, Y. Brechet, L. Legras, Mater. Sci. Forum 467–470 (2004) 629.
[13] L.G. Bell, AECL Report 1826, 1963.
[14] P. Bouffioux, N. Rupa, in: G.P. Gabol, G.D. Moan (Eds.), Zirconium in the Nuclear Industry 12th International Symposium, ASTM STP 1354, ASTM International, West Conshohocken, PA, 2000, p. 399.
[15] N. Rupa, M. Clavel, P. Bouffioux, C. Domain, A. Legris, in: G.D. Moan, P. Rudling (Eds.), Zirconium in the Nuclear Industry 13th International Symposium, ASTM STP 1423, ASTM International, West Conshohocken, PA, 2002, p. 811.
[16] Daigo Setoyama, Shinsuke Yamanaka, J. Alloy Compd 379 (2004) 193.
[17] Yong Hwan Jeong, Sang-Yun Park, Myung-Ho Lee, Byung-Kwon Choi, Jong-Hyuk Baek, Jeong-Yong Park, Jun-Hwan Kim, Hyun-Gil Kim, J. Nucl. Sci. Technol. 43 (2006) 977.
[18] D.O. Northwood, U. Kosasih, Int. Metals Rev. 28 (1983) 92.
[19] S. Banerjee, G.K. Dey, D. Srivastava, S. Ranganathan, Met. Mater. Trans. 28A (1997) 2201.
[20] R.N. Singh, R. Kishore, T.K. Sinha, B.P. Kashyap, J. Nucl. Mater. 301 (2002) 153.
[21] R.A. Oriani, P.H. Josephic, Acta Metall. 28 (1981) 669.
[22] M. Robertson, H.K. Birnbaum, Acta Metall. 34 (1986) 353.
[23] E. Sirosis, H.K. Birbhaum, Acta Metall. 40 (1992) 1377.
[24] Masato Ito, Kazuhira Ko, Hiroaki Muta, Masayoshi Uno, Shinsuke Yamanaka, J. Alloy Compd 446&447 (2007) 451.
[25] R.S.W. Shewfelt, Can. Met. Quart. 23 (1984) 441.
[26] N. Christodoulou, P.A. Turner, C.N. Tome, C.K. Chow, R.J. Klassen, Metall. Mater. Trans. 33A (2002) 1103.
[27] J. Fiela, J. Cadek, Mater. Sci. Eng. 75 (1985) 117.
[28] N. Prasad, G. Malakondaiah, P. Ramarao, Trans. Ind. Inst. Metals 42 (1989) S-165–S-174.
[29] Q.A. Ruano, J. Wadsworth, O.D. Sherby, Mater. Sci. Eng. 84 (1986) L1.